A Fiber Tracking Method for Building Patient Specific Dynamic Musculoskeletal Models from Diffusion Tensor Data

David I.W. Levin[1], Benjamin Gilles[1], Burkhard Mädler[2,3], and Dinesh K. Pai[1]

[1] Department of Computer Science
The University of British Columbia
Vancouver, British Columbia, Canada
[2] Philips Healthcare
[3] Department of Physics and Astronomy
The University of British Columbia
Vancouver, British Columbia, Canada

Abstract. A new musculoskeltal simulation primitive, the strand, can provide an efficient way of simulating complicated muscle fiber architectures [1]. In this paper we present a new fiber tracking algorithm based on an energy minimizing active curve that is well suited for building these strand type models from diffusion tensor imaging data. We present fiber tracking results for the Brachioradialis muscle in the left forearm of a male subject. The algorithm produces a space filling arrangement of fibers that are uniformly distributed throughout the muscle and aligned with the underlying muscle fiber direction.

Key words: musculoskeletal simulation, fiber tracking, diffusion tensor imaging

1 Introduction

Subject specific dynamic models of muscle can provide invaluable tools for the diagnosis of movement disorders [2] as well as for the study of the neurological control of movement [3]. Previous muscle simulations have focused on approaches such as line-of-force models and Finite Element Methods (FEM). However, line-of-force models overly simplify muscle fiber arrangement by treating muscles as straight lines and FEM models are complex to construct and time intensive to simulate. Recently a new simulation primitive, the muscle strand, has been developed for simulating musculotendon systems [1]. Strands are based on cubic spline curves with inertia. They allow contractile forces to be propagated along complex trajectories. By using strands to represent the arrangement of muscle fibers within a muscle we plan to construct accurate, efficient simulations which take into account subject specific fiber architectures. One major hurdle in building these strand-based models is the extraction of muscle fiber fields from subjects and the fitting of a number of strands to this data. In this paper we

present preliminary results of a semi-automatic technique for solving this problem using Diffusion Tensor Imaging (DTI) data from human muscle. Instead of relying on random seeding of the muscle volume to produce fiber paths we present an algorithm which seeks to fit a collection of energy minimizing, curves to the fiber field. Each of these contours could then be used as a strand in a musculoskeletal simulation.

2   Related Work

Musculoskeletal DTI has been previously used on human leg muscles. Sinha *et al.* [4] developed a tetrahedral gradient encoding scheme to perform fast DTI of human calf muscles. Lansdown *et al.* [5] used musculoskeletal DTI in order to measure pennation angle of muscle fibers in the human leg and compared the results to ultrasound (US) measurements. Lansdown found that the measurements acquired from the DTI data were statistically comparable to those from the US data.

Most fiber tracking approaches focus on seeding the DTI volume and using a numerical integration scheme to follow the primary eigenvector of the DTI tensor field to create a fiber path [6]. Probabilistic approaches have been used to deal with more complex fiber arrangements. Mori and Zijl have provided a summary of recent developments in fiber tracking [6]. Blemker and Delp presented a method for use with FEM muscle models that maps templated fiber geometries to anatomical meshes in order to include fiber data in the simulation. However these fiber templates are defined mathematically using tunable parameters, not from subject specific data [7].

3   Methods

Our pipeline for generating muscle geometry and patient specific strands begins with imaging the appropriate area of the body using MRI. Both anatomical and diffusion weighted scans are acquired. Muscle and bone surfaces are extracted from the anatomical scans while a muscle fiber field is computed from a DTI volume constructed from the diffusion weighted data. Below we present the details of each of these steps.

3.1   MRI Data Acquisition

Imaging for this study was performed on a 3T Philips Achieva MRI Scanner with dual nova gradients ($80mT/m$ maximum gradient strength, $200T/m/s$ maximum slewrate) and scanner software release 2.1.3.

During image acquisition the subject lay prone in the scanner with the left arm raised straight overhead to be placed as optimally as possible in the magnet's centre. The subject's forearm was secured in an 8-element phased array knee coil with $15cm$ inner diameter.

The imaging protocol consisted of a fast gradient echo T1W localizer for positioning and planning followed by low and high resolution T2W fast spin echo (FSE) scans for reconstruction of bone and muscle/fat surface boundaries. The session was concluded with a high resolution Diffusion Tensor Imaging (DTI) scan for muscle fiber orientation and segmentation.

Quick low resolution anatomical FSE-scans were acquired with an in-plane resolution of 1.5x1.5 mm^2 and a slice thickness of $4mm$ covering the entire lower arm (Fig.1).

The high resolution FSE was designed to match the Diffusion Tensor Imaging (DTI) scan in location, orientation and anatomy coverage with the following parameters: FSE-factor 12 with asymmetric profile order to give an effective echo time of TE=50ms; field of view (FOV):120x120x150 mm^3 with an in-plane resolution of 0.65x0.65 mm^2 and a slice thickness of $2mm$.

The lower resolution T2W-scan was used for segmenting bones and muscles that passed out of the field of view of the high resolution scan. Important parameters such as origin/insertion locations and bone coordinate systems could thus be obtained. Note that these two scans were run sequentially with the DTI scan and that the subject was immobilized. Therefore all volumes were closely aligned.

Diffusion Tensor Imaging (DTI) was performed with a single shot diffusion sensitized spin-echo Echo Planar Imaging (EPI) sequence involving 16 different gradient encoding directions at a maximum diffusion b-value of 500s/mm^2. We used a reduced FOV of 120x120x150mm^3, SENSE-factor of 2.0 and enhanced gradient performance to shorten the echo train length of the EPI-readout as much as possible for better compensation of susceptibility induced artifacts. Fat suppression was performed with a spectral spatial inversion prepared fat suppression technique. Further imaging parameters were as follow: TE=48ms, TR=6000ms, acquisition matrix 80x80 leading to an effective acquisition voxel size of 1.5x1.5x2.0 mm^3 and a scan time of 5 minutes.

3.2   Segmentation of Bone and Muscle Surfaces

Given the high complexity of the forearm structure and the fuzzy muscle boundaries on MRI (e.g. because of thin intermuscle fat), surfaces are not reconstructed based on a slice-by-slice segmentation. Instead, the subject-specific model is obtained from the registration of a template surface onto the individual MRI. This prior model was constructed from the Ultimate Human Dataset (Snoswell Design, Adelaide).

Musculoskeletal registration is particularly challenging because it involves a large number of interrelated components undergoing large non-linear deformations with large anatomical variations in the population. Hence allowable deformations need to be carefully parameterized to avoid falling into one of the numerous local solutions, *and* to present sufficient degrees of freedom [8, 9].

Our surface-to-image registration method is based on discrete deformable models evolving under internal forces (e.g., elastic forces) and external forces

(e.g., image forces, user constraints). Our internal forces enforce a spatially co-herent evolution and consistent shapes by minimizing non-rigid local transfor-mations between the model and the template. Our method is derived from a fast deformation technique called *shape matching* developed in the computer graphics community [10, 11], to efficiently approximate large soft-tissue elastic deformations. In [12], we show that quasi automatic inter-patient registration can be achieved when the template is built from a reference image dataset (ex-ternal forces locally match icons around the surface). In this present work, we do not have any prior appearance model, so external forces are based on user constraints (for each bone/ muscle, the user places internal/ external/ frontier points on MRI slices) and local gradient maximization. The model ($\sim 20k$ parti-cles) can be deformed in real time, so the adaptation is done interactively while putting constraint points.

3.3   DTI Data Processing and Fiber Tracking

In order to reduce distortion in the diffusion weighted images, eddy correction was performed using FMRIB's Diffusion Toolbox (FDT) [13]. Image volumes were converted from DICOM to Analyze format in order to perform the correc-tion. MedINRIA's DTI Track [14] was used to compute a tensor image from the diffusion weighted data. MATLAB was used to compute the primary eigenvector of each tensor in order to facilitate fiber tracking.

The fiber tracking performed in this study differs from typical tractography algorithms because of the end use of the data. We are seeking to build a strand-based dynamic model from the diffusion tensor data (DTI). The algorithm seeks to evenly distribute a user-specified number of strands within the segmented muscle surface. In order to accomplish this we utilize a deformable contour for fiber tracking and segmentation. In general this method shares similarities with active contours used for image segmentation [15]. However instead of segmenting the boundary of the muscle we seek a space filling arrangement of curves which lie both on and inside the muscle surface. The algorithm is semi-automatic in that it requires the user to specify the insertion and origin of the muscle to which tracking will be applied. A template strand is initialized between the insertion and origin points and the user can move control points on the template to ensure that the template strand is entirely enclosed by the muscle surface. Once this initialization step is complete, the required number of strands are initialized to be identical to the template strand. Each strand is discretized using linear elements.

The energy for this i^{th} element is

$$E^i = \alpha \|\mathbf{x}_1^i - \mathbf{x}_0^i\|^2 - \beta \left(|\mathbf{e}^i \cdot \mathbf{t}\left(\mathbf{x}_m^i\right)| \right) + \gamma E_r^i, \tag{1}$$

where $\mathbf{x}_j^i$ are the end points of element i, $\mathbf{e}^i$ is the normalized element tangent vector, $\mathbf{t}\left(\mathbf{x}_m^i\right)$ is value of the underlying primary eigenvector evaluated at the midpoint of the element and E_r^i is a repulsion energy.

The initial term in the energy equation is a stiffness term and prevents un-necessary elongation of the strand during tracking. The second term causes each

element of the strand to align with the underlying DTI fiber field. The final term is a repulsion term that is computed between a strand and all other neighboring strands. This term forces the strands away from each other thus seeking a space filling configuration within the muscle surface.We seek the minimum energy configuration of all strands subject to the constraints that each node of a strand must lie inside or on the muscle surface. The constraints that arise in such a problem are quite complicated. Formulating the minimization at the velocity level is easier because the constraints can be locally linearized. The following equation is arrived at by linearizing equation (1) and adding a kinetic energy term.

$$Q\left(\dot{\mathbf{x}}\right) = h\dot{\mathbf{x}} \cdot \bigtriangledown E^s + \dot{\mathbf{x}} \cdot \dot{\mathbf{x}}, \tag{2}$$

where h is the algorithm time step, $\bigtriangledown E^s$ is the negative force acting on strand s and can be computed from the sum of the gradients of E^i and $\dot{\mathbf{x}}$ is a vector of the strands nodal velocities.

We minimize Q subject to the constraints in order to obtain a feasible velocity, and step the solution forward in time. An initial perturbation is applied to each strand to prevent the repulsion term from being infinite. In this implementation the force term is evaluated using an explicit trapezoidal type sum. Nodal velocities are computed from these forces using QL, a robust program for solving quadratic programming problems subject to equality and inequality constraints [16]. The computed nodal velocities are then applied to the nodal positions and the process is repeated until the strands reach a steady state.

Equality constraints are used to fix the insertion and origin points of each strand in space, and inequality constraints are used to keep strand nodes inside the muscle surface. Ray-triangle intersection is used to detect if a node has violated the muscle surface constraint. If so the node is moved back to the surface and an inequality constraint is added to prevent the node from moving in a direction normal to the triangle that it passed through.

4   Results and Discussion

In this section we present the preliminary results of muscle segmentation and fiber fitting for the Brachioradialis muscle of the left arm of the subject.

Despite a careful placement of constraint points, the anatomical segmentation is not perfect, because of fuzzy edges and partial volume effects. We also expect small misalignments between the different volumes due to slight movements of the subject. Although more validation and cross-comparison between different manual segmentations will be required, we presume for the moment that our segmentation lies within a $3mm$ error bound in terms of distance to the surfaces. Fig. 1 also shows how the segmentation of the Brachioradialis is constrained by the boundaries of other forearm muscles.

An initial example (Fig. 2) demonstrates how the deformable curves take muscle fiber vector field information into account during the fiber tracking process. Without vector field information the curves fill the entire muscle shape.
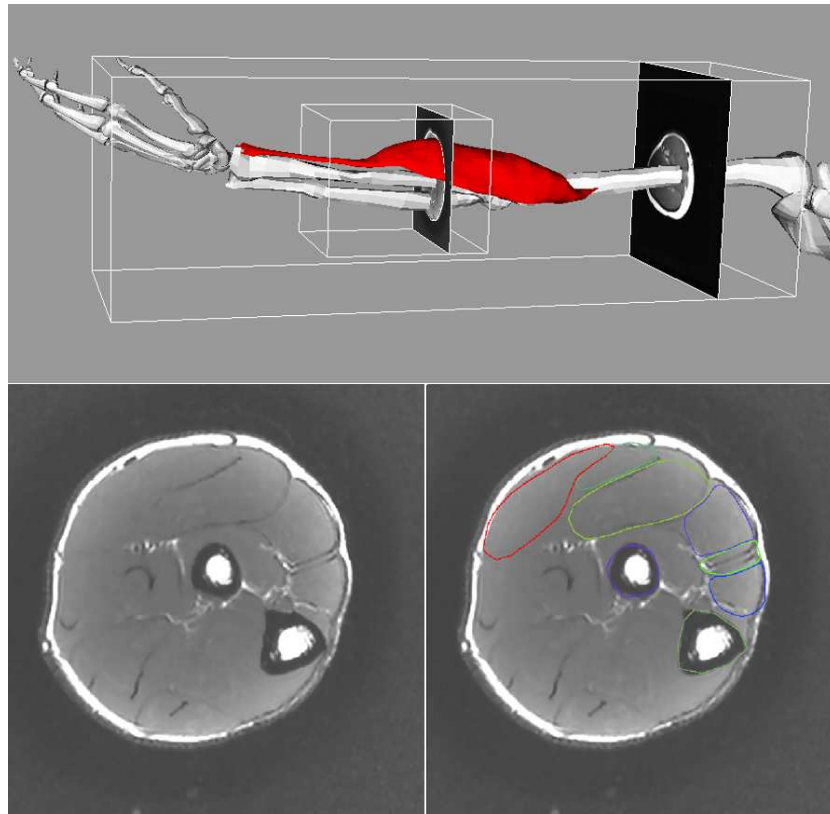
Fig. 1. Left: High/ low resolution MRI volumes and reconstructed models (bones and Brachioradialis muscle) of the arm. Bottom: High resolution sample slice with and without superimposed models. Note that the Brachioradialis is shown in red while other muscles in the forearm are shown as contours of different colours.
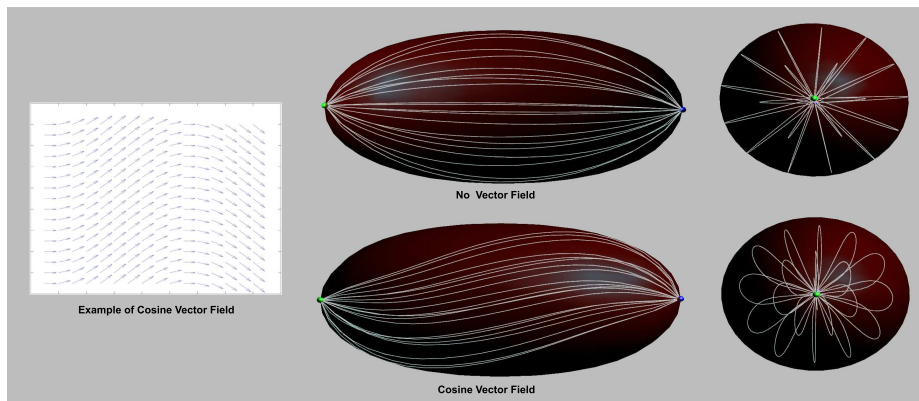
Fig. 2. A simple example showing how the curves respond to vector data. The upper images show an ellipsoidal shape filled with curves using no muscle vector field information. The lower images show the same curves under the influence of a cosine vector field.
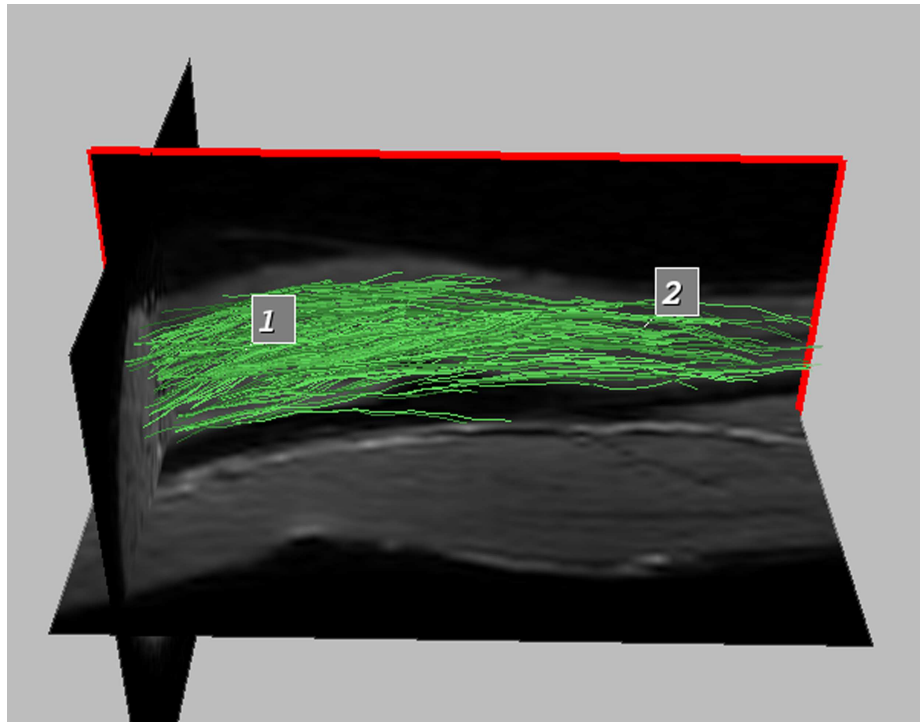
Fig. 3. DTI Fiber Tracking of the Brachioradialis muscle.

Incorporating vector field information still leads to a uniform distribution of strands within the muscle but their configuration is altered noticeably.

Next we show the results of tractography performed using the Stanford DTI Query tool (Fig. 3). The pathway shown was segmented using two volumes-of-interest positioned in the region of the Brachioradialis muscle. The primary eigenvectors of the DTI data used to compute this pathway were used to build the muscle vector field for the strand fiber tracking algorithm.

Parameters for the strand tracking algorithm were adjusted manually until we could achieve a space filling configuration of strands for which the average dot product between a strand element and the muscle fiber direction vector was 0.9 or greater. This led to parameter values of 0.5 for α, 20 for β and 300 for γ. We used a time step (h) of 0.01. Fig. 4 shows the output of the strand fiber tracking algorithm. The top left image shows the segmented muscle mesh of the Brachioradialis muscle and the template strand. The insertion and origin of the muscle are shown as green and blue spheres respectively. Notice that as the algorithm progresses that the strand arrangement (shown by the white lines) progresses from being tightly packed along the medial axis of the muscle to being evenly distributed throughout the whole muscle geometry. Also note that despite the extreme narrowing of the muscle the strands remain constrained inside the muscle shape. Fig. 5 shows the fiber field matching behavior of one strand from the fiber tracking result. Each colored line shows the direction of the muscle fiber field at the midpoint of each strand midpoints. Notice that once the strand reaches its final configuration all the vectors are virtually parallel with the elements (average dot product with the fiber field equal to 0.95) showing that the contour does align itself with the underlying fiber field.
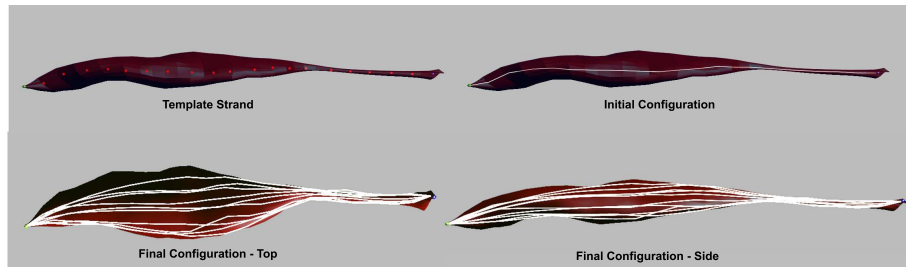
Fig. 4. The progression of the fiber tracking algorithm from the initial template strand (top left) to the completed strand configuration (bottom).

In terms of future work, parameter optimization for the energy term needs to be performed in order to find values that fit a wide range of fiber configurations accurately. Also necessary is the modification of the algorithm so that it can be used on non-fusiform muscles. Furthermore, though our preliminary results are encouraging, rigorous validation of the algorithm needs to be conducted using
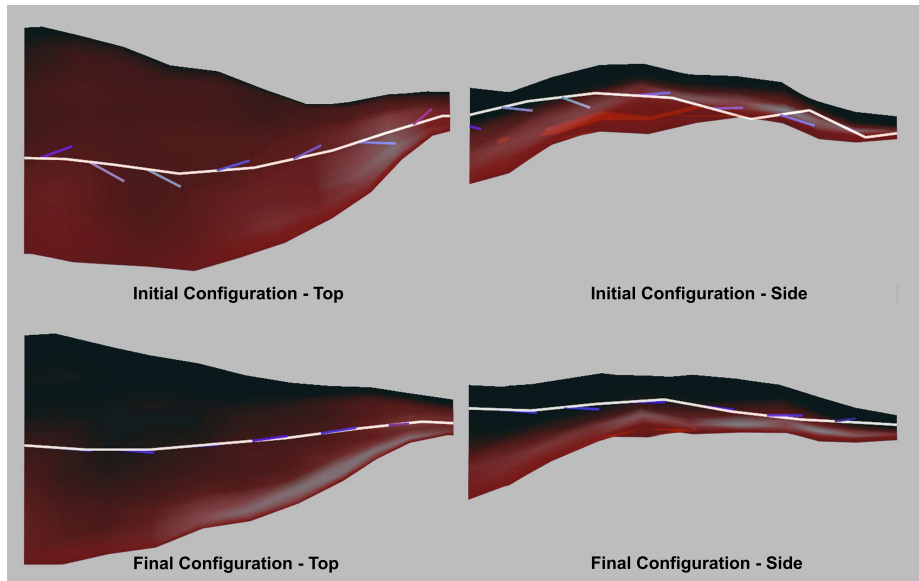
Fig. 5. The fiber field matching behavior of one of the strands from the muscle fiber tracking. Colored lines show the direction of the fiber field at each element midpoint.

more subjects. Ultimately we hope to build numerous dynamic muscle models and explore the effect that differing fiber architecture has on behavior of muscles.

5   Conclusion

We have developed a fiber tracking algorithm which fits a finite number of muscle strands to a muscle fiber field using an energy minimizing approach. Unlike previous tractography approaches, this algorithm allows more careful control of the number of muscle strands produced by the algorithm and is thus well suited for building patient specific, strand-based dynamic muscle models.

6   Acknowledgements

7   References

References

1. Sueda, S., Kaufman, A., Pai, D.K.: Musculotendon simulation for hand animation. ACM Trans. Graph. (Proc. SIGGRAPH) **27**(3) (2008) 83:1–83:8
2. Piazza, S.J., Delp, S.L.: The influence of muscles on knee flexion during the swing phase of gait. Journal of Biomechanics **29**(6) (1996) 723–733
3. Thelen, D.G., Anderson, F.C., Delp, S.L.: Generating dynamic simulations of movement using computed muscle control. Journal of Biomechanics **36**(3) (2003) 321–328
4. Sinha, S., Sinha, U., Edgerton, V.R.: In vivo diffusion tensor imaging of the human calf muscle. Journal of Magnetic Resonance Imaging **24**(1) (2006) 182–190
5. Lansdown, D.A., Ding, Z., Wadington, M., Hornberger, J.L., Damon, B.M.: Quantitative diffusion tensor MRI-based fiber tracking of human skeletal muscle. J Appl Physiol **103**(2) (2007) 673–681
6. Mori, S., van Zijl, P.C.M.: Fiber tracking: principles and strategies - a technical review. NMR in Biomedicine **15**(7) (2002) 468–480
7. Blemker, S.S., Delp, S.L.: Three-dimensional representation of complex muscle architectures and geometries. Annals of Biomedical Engineering **33** (2005) 661–673
8. Maintz, J., Viergever, M.: A survey of medical registration. Medical image analysis **2**(1) (1998) 1–36
9. Blemker, S., Asakawa, D., Gold, G., Delp, S.: Image-based musculoskeletal modeling: Applications, advances, and future opportunities. Journal of Magnetic Resonance Imaging **25**(2) (2007) 441–451
10. Müller, M., Heidelberger, B., Teschner, M., Gross, M.: Meshless deformations based on shape matching. Proc. of SIGGRAPH'05 (2005) 471–478
11. Rivers, A., James, D.: Fastlsm: Fast lattice shape matching for robust real-time deformation. Proc. of SIGGRAPH'07, ACM Transactions on Graphics **26**(3) (2007)
12. Gilles, B., Pai, D.K.: Fast musculoskeletal registration based on shape matching. Proc. of MICCAI'08 (2008) 822–829
13. FMRIB: Fmrib's diffusion toolbox - fdt v2.0. Webpage: `http://www.fmrib.ox.ac.uk/fsl/fdt/index.html` (2007)
14. INRIA: MedINRIA. Webpage: `http://www-sop.inria.fr/asclepios/software/MedINRIA/` (2006)
15. Kass, M., Witkin, A., Terzopoulos, D.: Snakes: Active contour models. International Journal of Computer Vision **1**(4) (1988) 321–331
16. Schittkowski, K.: QL: A fortran code for convex quadratic programming - user's guide. Report for the Department of Mathematics, University of Bayreuth (2003)